Molecular Motions within the Pore of Voltage-Dependent Sodium Channels

Jean-Pierre Bénitah,* Ravi Ranjan,# Toshio Yamagishi,* Maria Janecki,* Gordon F. Tomaselli,* and Eduardo Marban*

*Section of Molecular and Cellular Cardiology, Department of Medicine, and #Department of Biomedical Engineering, Johns Hopkins University School of Medicine, Baltimore, Maryland 21205 USA

ABSTRACT The pores of ion channel proteins are often modeled as static structures. In this view, selectivity reflects rigidly constrained backbone orientations. Such a picture is at variance with the generalization that biological proteins are flexible, capable of major internal motions on biologically relevant time scales. We tested for motions in the sodium channel pore by systematically introducing pairs of cysteine residues throughout the pore-lining segments. Two distinct pairs of residues spontaneously formed disulfide bonds bridging domains I and II. Nine other permutations, involving all four domains, were capable of disulfide bonding in the presence of a redox catalyst. The results are inconsistent with a single fixed backbone structure for the pore; instead, the segments that line the permeation pathway appear capable of sizable motions.

INTRODUCTION

Evolution has produced a variety of ion channel proteins that reconcile the seemingly contradictory demands of a high flux rate on one hand and exquisite selectivity on the other. Sodium channels epitomize this evolutionary balancing act. These proteins select sodium over all other biological ions by one or more orders of magnitude, yet support flux rates that are very nearly diffusion-limited (Hille, 1992). Remarkably little is known about the molecular strategies that ion channels use to transport ions rapidly but with fine discrimination. Biophysical approaches have led to the prevailing concept that selectivity arises either from specific binding of ions to pore-lining residues, molecular sieving, or both (Armstrong, 1989). It is generally assumed that the pore must be fairly rigid to preserve selectivity (Eisenman and Krasne, 1975). Nevertheless, biological proteins are known to undergo substantial internal motions, ranging from side-chain realignments on a picosecond time scale to large folding transitions occurring over several microseconds or more (Brooks et al., 1988; Levitt, 1989). Indeed, recent mutagenesis studies have revealed major internal motions during the gating of sodium channels: upon depolarization, the S4 voltage sensors move 4.5–11 Å within ~1 ms (French et al., 1996). However, gating is much slower than permeation. No experimental data are available to define the mobility of the regions of the channel that mediate ion translocation.

It is challenging to devise means of quantifying motions within proteins of unresolved structure, such as sodium channels. Several general principles of intramolecular bond formation serve as useful starting points. In particular, disulfide bonds can form only when thiol side chains collide, such that the β carbons of two cysteine residues come within 4.6 Å of each other (Srinivasan et al., 1990; Careaga and Falke, 1992; Careaga et al., 1995). Disulfide formation is a collisional process: the more frequently two thiols collide, the more likely they are to form a bond. Thus disulfide formation rates in proteins engineered to contain two cysteines at known sites in the primary structure can be used to measure the collisional frequency of those cysteines. This approach, called disulfide trapping, has been used successfully to probe the dynamics of various proteins (Falke and Koshland, 1987; Careaga and Falke, 1992; Careaga et al., 1995). The ability to form disulfide bonds implies at least occasional proximity, and the kinetics of bond formation provides an index of the amplitude and rate of internal motions. Application of this approach to a chemosensory galactose receptor of known crystal structure has revealed large motions of various residues on the surface of the protein (Careaga and Falke, 1992; Careaga et al., 1995).

MATERIALS AND METHODS

Mutagenesis and channel expression

In vitro site-directed mutagenesis is performed on the double-stranded rat skeletal μ1 Na^+ channel α-subunit (Trimmer et al., 1989), using *Pfu* DNA polymerase (Weiner et al., 1993). The regions spanning the mutation sites were then verified by DNA sequencing. After in vitro transcription utilizing SP6 RNA polymerase, cysteine mutants were coexpressed with β1 subunit cRNA (Isom et al., 1992) by injection into stage V or VI *Xenopus laevis* oocytes as previously described (Tomaselli et al., 1995). When expressed in oocytes, the E755C mutant expressed small currents with inconsistent Cd^{2+} block affinities; this mutant was rederived de novo in the mammalian expression CMV promoter-based vector pGW1H (British Biotechnology, Oxford, England) and expressed transiently in HEK-293 cells (Kamp et al., 1996) to obtain the single-mutant Cd^{2+}-binding data in Fig. 3.

Received for publication 3 March 1997 and in final form 16 May 1997.

Address reprint requests to Dr. Eduardo Marban, Section of Molecular and Cellular Cardiology, 844 Ross Building, The Johns Hopkins University School of Medicine, Baltimore, MD 21205. Tel.: 410-955-2776; Fax: 410-955-7953; E-mail: marban@welchlink.welch.jhu.edu.

0006-3495/97/08/603/11 $2.00

Electrophysiology

Macroscopic currents were recorded using a two-microelectrode voltage clamp (OC-725B; Warner Instrument Corp., Hamden, CT) 2–5 days after RNA injections at room temperature (20 ± 2°C). Both the voltage-sensing and current-passing electrode were filled with 3 M KCl. Whole-cell currents were measured in modified frog Ringer's solution (ND-96) containing 96 mM NaCl, 2 mM KCl, 1 mM $MgCl_2$, and 5 mM HEPES (pH 7.6). In experiments where the Na^+ concentration was decreased, NaCl was substituted isosmotically with sorbitol. To measure the affinities for cadmium block, $CdCl_2$ was added to the ND-96 solution from a stock of 500 mM in H_2O, in concentrations ranging from 50 nM to 10 mM. Reduced glutathione and dithiothreitol (DTT) were dissolved directly in the extracellular solution at a concentration of 1 mM just before use. Redox catalyst $Cu(II)(1,10\text{-phenanthroline})_3$ stock solution was prepared according to the method of Careaga and Falke (1992) by dissolving 150 mM $Cu(II)SO_4$ and 500 mM 1,10-phenanthroline in a 4:1 water/ethanol solution. This stock solution was diluted to 100 μM concentration in ND-96 at the time of use.

Data analysis

Whole-cell currents were sampled at 5 kHz through a 12-bit A/D converter (model TL-1 DMA Labmaster; Axon Instruments, Foster City, CA) and low-pass-filtered at 1–2 kHz (−3 dB) with an 8-pole Bessel filter (Frequency Devices, Haverhill, MA). The currents were acquired and analyzed with custom-written software as previously described (Bénitah et al., 1996). The current-voltage relationships were obtained by a series of 50-ms voltage clamp depolarizations with a 5-mV increment from a −100-mV holding potential to membrane potentials up to +20 mV, applied at 2-s intervals. The time course of external solution changes was determined by monitoring the peak inward current elicited by 50-ms depolarizations from −100 mV to −30 or −20 mV every 5 s, while the bath solution was being changed from 96 to 48 mM Na^+ pulsing to the peak current potential, in steps lasting 50 ms and applied every 5 s. Current was measured as the difference between the peak current and the current level at the end of the pulse. Best-fit curves to the data were determined by a nonlinear least-squares method (Levenberg-Marquardt algorithm; Origin, MicroCal, Northhampton, MA).

Molecular modeling

The molecular model of the μ1 Na^+ channel was made using the software programs Insight and Discover (Biosym/MSI, San Diego, CA) and Sculpt (Interactive Simulations, San Diego, CA). The model comprises 11 residues in each of the four domains: L396 to F406 in domain I, I751 to W761 in domain II, V1233 to M1243 in domain III, and I1525 to L1535 in domain IV. After developing the amino acid sequence for four domains in Insight, the accessibility and the z (perpendicular to the plane of the membrane) distance data (Chiamvimonvat et al., 1996a) were used to make the loop structure with Sculpt. Discover was used to energy-minimize the structure, with the distances between the residues that exhibit disulfide bonds when mutated to cysteine as additional constraints. As the z distance, accessibility, and interatomic distance were available for only the four central residues in each domain, the three to four residues at the ends of each domain were not constrained in space. The positions of these end residues were based solely on the computational results obtained from the energy minimization calculation.

RESULTS AND DISCUSSION

To probe the mobility of the sodium channel pore, we introduced pairwise cysteine substitutions into the pore-lining (P) segments. Two cysteinyl side chains can form metal-chelating sites if and only if they are in close proximity in the folded protein; disulfide bonds can form if and only if the protein dynamics enable the two side chains to collide (Liu et al., 1996; Bénitah et al., 1996; Zhang et al., 1996; Krovetz et al., 1997). Fig. 1 shows a cartoon of the channel highlighting the residues that were substituted by cysteine, individually and in pairs. We focused particularly on those positions that determine the selective permeability of this channel (Terlau et al., 1991; Heinemann et al., 1992; Favre et al., 1996; Chiamvimonvat et al., 1996a,b; Pérez-García et al., 1997). Each of the boxed cysteinyl mutants was paired with substitutions in the other three domains to create a total of 21 distinct double mutants.

Disulfide bridge formation in the pore region of the channel can reasonably be expected to produce changes in conductance. Fig. 2 shows a striking confirmation of this prediction. Oocytes injected with RNA for the D400C + E755C double mutant had no detectable ionic current when superfused by normal ND-96 solution, which was oxidized by virtue of equilibration with ambient O_2 (Fig. 2 *A*, *a*). Exposure to the reducing agent dithiothreitol (DTT) rapidly revealed a voltage-dependent inward current (Fig. 2 *A*, *b*). This effect occurred quickly, reaching a maximum within 2 min, and could be completely reversed after switching back

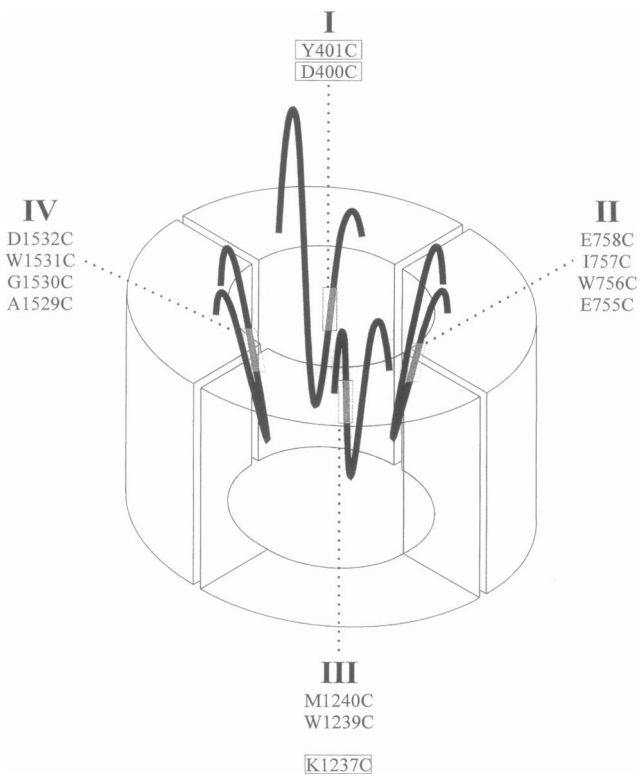

FIGURE 1 Cartoon of the μ1 skeletal muscle sodium channel α-subunit. The P segments (*bold*) of each of the four domains are arranged like the staves of a barrel around a central ion conduction pore. The cysteinyl mutations of the amino acid side chains characterized in this study are shown. Numbering of amino acid residues corresponds to their position in the sequence. The naturally variant position in the domain I P segment, Y401, and the putative selectivity filter residues of domains I and III, D400 and K1237, were chosen as double-mutant pivots; these are highlighted by boxes. The standard single-letter amino acid designations are used.

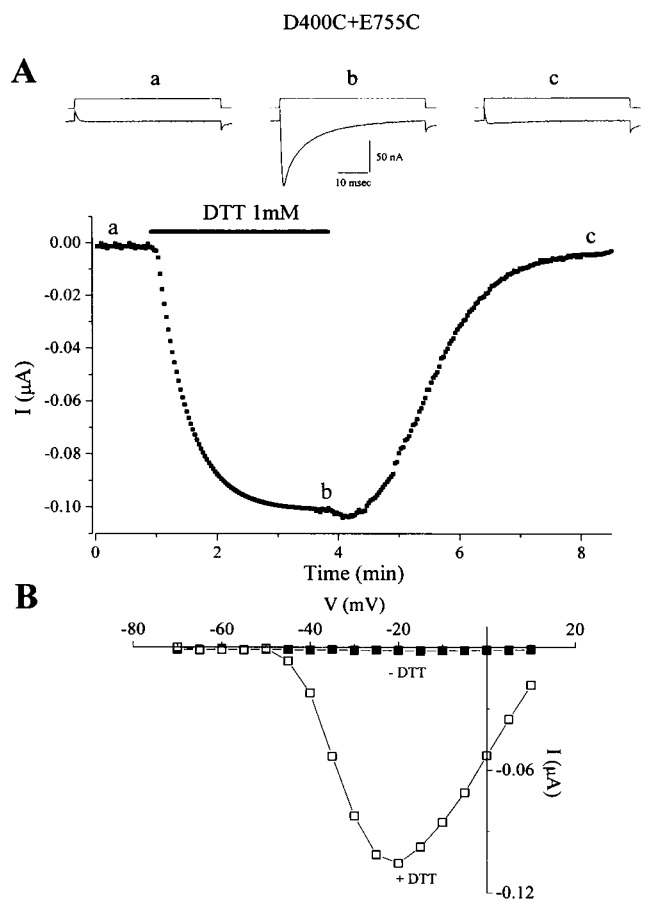

FIGURE 2 Evidence for spontaneous formation of a disulfide bond between D400C and E755C and time course of current development during exposure to DTT. Under normal oxidizing conditions, no macroscopic membrane current could be recorded from oocytes injected with the cRNA encoding this double mutant. The solid bar indicates the period of 1 mM DTT application. The current dramatically and reversibly increased in a reducing environment. The upper panels show current traces elicited by 50-ms pulses from −100 to −20 mV repeated at 2-s intervals, before (*a*), during (*b*), and after (*c*) the addition of 1 mM DTT dissolved in solution. (*Bottom*) Current-voltage relationship for D400C + E755C in control conditions (■) and after 3 min of exposure to 1 mM DTT (□).

to the control oxidized environment. The current records (Fig. 2 *A*, *b*) and current-voltage relationships (Fig. 2 *B*) demonstrate that the redox-sensitive channels gate normally in the presence of DTT. Similar results were obtained by using another reducing agent, reduced glutathione. We interpret these results as evidence for a spontaneous disulfide bond bridging the 400 and 755 positions and completely occluding the pore. It has been proposed (Terlau et al., 1991; Heinemann et al., 1992; Chiamvimonvat et al., 1996a,b; Favre et al., 1996; Pérez-García et al., 1997) that these aspartate and glutamate residues, along with K1237 and A1529 (DEKA ring), form the sodium channel "selectivity filter." Based on the dimensions of the ion-selective region of the Na^+ channel suggested by organic cation size exclusion (Hille, 1992), we expected that multiple pairs of cysteine-substituted selectivity residues (DEKA) would be capable of forming disulfide bonds. Such was not the case. D400C + E755C was unique among five DEKA pairs examined (the others being D400C + K1237C, D400C + A1529C, E755C + K1237C, and K1237C + A1529C) in exhibiting a redox-sensitive conductance.

The whole-cell current was not affected by DTT or reduced glutathione in any of the other double (or single) mutant Na^+ channels. Nevertheless, it is possible that some bridges had formed in a narrow region of the pore not accessible to those reducing agents. We thus used a complementary approach to detect vicinal cysteinyls, namely the analysis of sensitivity to block by group IIb divalent cations such as Cd^{2+} (Bénitah et al., 1996; Krovetz et al., 1997). Fig. 3 summarizes the results of free energy analysis for Cd^{2+} binding to single ($\Delta\Delta G_X$, $\Delta\Delta G_Y$) and double ($\Delta\Delta G_{X,Y}$) mutants. If metal binding were cooperative, any given pair would display excess free energy as compared to the sum of the single mutants of which it is composed (Wells, 1990); data points for such double mutants would lie below the line of identity (*dashed line* in Fig. 1 *C*). Most double mutants yielded simply additive free energies for Cd^{2+} block, with three notable exceptions. First, Y401C + G1530C forms a high-affinity Cd^{2+} binding site; as we have previously argued, these residues are so close to each other that they bind Cd^{2+} cooperatively (Bénitah et al., 1996). Second, the spontaneous disulfide between Y401C and E758C exhibits a low Cd^{2+} block affinity until it is reduced, at which point a high-affinity Cd^{2+}-binding site is revealed (Bénitah et al., 1996). Third, D400C + E755C, which forms functional channels only in a reduced environment (Fig. 2), exhibits marked cooperativity with an excess free energy of >5 kcal/mol. Two of these three mutants that bind Cd^{2+} cooperatively also spontaneously form disulfides. Thus both observations support the idea that these pairs (401 + 758, 400 + 755) are particularly closely apposed within the sodium channel.

Residues in more mobile parts of a protein may interact only transiently; it is known that only a small fraction (~1 in 10,000) of side-chain collisions result in disulfide bond formation (Careaga and Falke, 1992). Nevertheless, fluctuations in protein structure can be trapped by disulfide bond formation in the presence of a redox catalyst such as copper phenanthroline [Cu(II)(1,10-phenanthroline)$_3$, abbreviated hereafter as Cu(phen)$_3$; (Careaga and Falke, 1992)]. To determine whether any of the mutant pairs were capable of forming catalyzed disulfides, we exposed channels to Cu(phen)$_3$. Disulfide formation under these conditions, evident as redox-sensitive changes in current magnitude, implies motion of the P segments. In preliminary experiments we found that oocytes become leaky when exposed to high concentrations (≥1 mM) of Cu(phen)$_3$, but concentrations of 100 μM or less have no effect on wild-type or single-mutant channels. This contrasts with the behavior in Fig. 4 *A*; here, current through Y401C + G1530C channels rapidly decreased after the addition of 100 μM Cu(phen)$_3$. Recall that this pair binds Cd^{2+} cooperatively without spontaneously forming a disulfide bond. The inhibitory effect

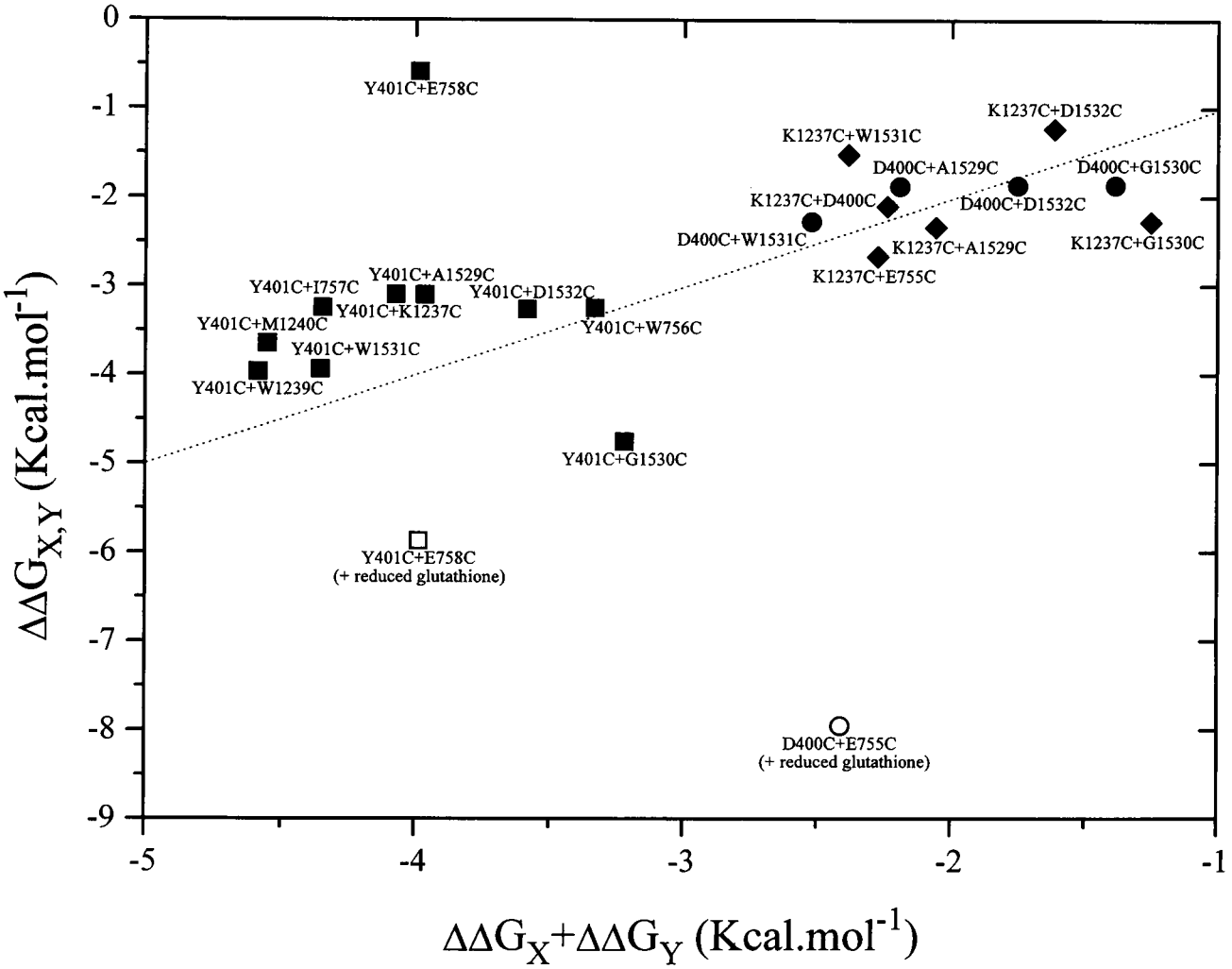

FIGURE 3 Free energy analysis for Cd^{2+} binding in double-cysteine mutants. Plot showing the changes in the sum of free energies of Cd^{2+} binding for component single mutants X and Y ($\Delta\Delta G_X + \Delta\Delta G_Y$) versus free energies of binding for the corresponding double mutant ($\Delta\Delta G_{X,Y}$). The dotted line represents the line of unity. A point on or near this line of identity indicates no interaction of the substituted cysteines. Large deviations (>1 kcal mol^{-1}) from the line of identity reveal positive (*under the line*) or negative cooperativity for Cd^{2+} binding. Each symbol represents a different fulcrum position: ■, □, Y401C; ●, ○, D400C; and ◆, K1237C.

was equal at all test potentials (data not shown), ruling out a simple voltage shift. Fig. 4 shows additional evidence that the reduction of the current is not due to a nonspecific effect such as an alteration of the surface charge; in Fig. 4 *A*, the current does not recover spontaneously upon washout of the redox catalyst. However, application of DTT (1 mM, Fig. 4 *B*) does reverse the effect of $Cu(phen)_3$, albeit slowly. These observations support the idea that the 401 + 1530 residue pair has been driven to form a disulfide bridge; when bridged, the channels are nonconducting. DTT breaks the bonds and restores ion flux through the channels.

Catalyzed intersubunit disulfide bonds involving residues in the outer mouth of *Shaker* K^+ channels form at an appreciable rate only when the channels undergo C-type inactivation (Liu et al., 1996). The results in Fig. 4, *C* and *D*, argue against strongly voltage-dependent reactions in Y401C + G1530C channels. The channels were exposed to $Cu(phen)_3$ for several minutes, either in the closed state while the oocyte was held at −100 mV (Fig. 4 *C*), or in inactivated states holding at −20 mV (Fig. 4 *D*). The inhibition of the current after washout was equivalent to that seen with repetitive depolarizing pulses (Fig. 4, *A* and *B*). Many other cysteine pairs can be induced to form disulfides when a redox catalyst is added (Fig. 6 *A*, *dashed arrows*). Nevertheless, application of protocols like that in Fig. 4, *C* and *D*, to all other bondable pairs similarly failed to elicit any evidence for voltage dependence of the reactions. Although we cannot exclude subtle differences in reaction rates based on these results, our experiments argue that disulfide formation is not inhibited by maintaining the channels in resting or inactivated states.

It is not surprising that the 401 + 1530 pair is capable of bridging, given previous evidence of proximity based on Cd^{2+}-binding cooperativity (Fig. 3; Bénitah et al., 1996).

However, 401 + 1530 was by no means unique in its ability to form a catalyzed bond. Fig. 6 *A* summarizes the results. Each panel shows one particular fulcrum residue (*enclosed in a box*) and the other mutants with which it was paired; solid arrows connect those residues that spontaneously formed disulfides, and dashed arrows those that bridged only in the presence of $Cu(phen)_3$. In all, disulfide formation was observed for 11 of the 21 engineered cysteine pairs (two spontaneous, nine catalyzed). Just as interesting was the observation that other engineered cysteine pairs yielded no detectable or specific effect of the $Cu(phen)_3$; these are depicted by unconnected residues in each panel of Fig. 6 *A*. We conclude that these unconnected pairs of residues rarely if ever collide with each other. The alternative possibility that some disulfides do form but are nonperturbing (Chervitz et al., 1995) seems unlikely, given that all of these positions (with the sole exception of W756) significantly alter permeation and block when mutated individually to cysteine (Chiamvimonvat et al., 1996a).

The results are surprising in that disulfide bonding is widespread, yet specific. The 401 position in domain I is particularly promiscuous, capable of pairing with at least one residue in each of the three other domains (758 and 757 in II, 1239 in III, and 1532 and 1530 in IV). This finding implies that the region of the P segment that 401 inhabits must be quite mobile. In contrast, the residues of the putative selectivity filter are more constrained. The DEKA residues have been proposed to form a coordinated, symmetrical ring around the narrowest part of the pore (Lipkind and Fozzard, 1994; Guy and Durell, 1995). Such structural models predict that all pairwise permutations of the DEKA positions would be capable of cross-linking, assuming minimal mobility to satisfy the angular requirements for disulfide bond formation (Srinivasan et al., 1990). Instead, all but one of such combinations (K1237C + D400C, K1237C + E755C, and D400C + A1529C) fail to form bonds. The present findings argue against the idea of a DEKA selectivity filter. Chiamvimonvat et al. (1996b) had previously questioned this concept, based on analysis of single cysteine mutants (as confirmed by Tsushima et al., 1997).

Several domain IV mutants (G1530C, W1531C, and D1532C) altered ionic selectivity more than did the DEKA site substitutions E755C or A1529C (Chiamvimonvat et al., 1996b). The present data again support a special role for the 1530–1532 positions. The conclusion that there is extensive motion within the Na^+ channel P segments does not necessarily imply unconstrained flexibility, which would likely produce nonspecific patterns of interaction. We find instead distinctive hot spots and absences in pairing ability within individual P segments. For example, position 400 can bond with 1530, 1531, and 1532, but not with 1529. In contrast, 1237 interacts selectively with 1530 and 1531, skipping 1529 and 1532. The mobilities of individual residues vary considerably and obey specific spatial constraints.

To estimate the amplitudes of the motions at each position, we measured the kinetics of disulfide bond formation (Careaga and Falke, 1992). The rate of disulfide bond formation, k_{ss}, was measured according to the following reaction scheme:

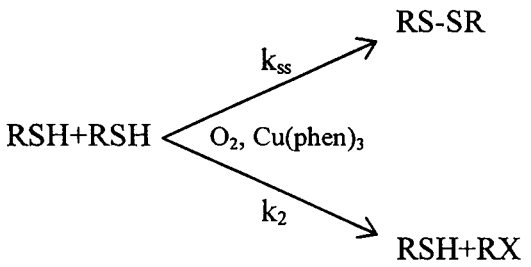

Assuming a first-order reaction $f(t)$, the rate constants of the disulfide reaction (k_{ss}) and of the competing reaction (k_2) yielding higher oxidation products of cysteine (Oae, 1991) are as follows:

$$f(t) = \frac{k_{SS}}{k_{SS} + k_2} \cdot [1 - e^{-(k_{SS}+k_2)\cdot t}] \qquad (1)$$

We corrected the observed reaction kinetics for the rate of bath exchange in our perfusion system determined by the time course of current reduction after a decrease in Na^+ concentration from 96 to 48 mM (Fig. 2 *E*; NaCl was substituted isosmotically with sorbitol). The time course of external solution changes was determined by monitoring the peak inward current elicited by 50-ms depolarizations from −100 mV to −30 or −20 mV every 5 s. This process was well-fit by a single exponential of time constant t_p. Thus Eq. 1 can be transformed to

$$f(t) = \frac{k_{SS}}{k_{SS} + k_2} \cdot [1 - e^{-(k_{SS}+k_2)\cdot (t+\{t_p \cdot e^{-w_{t_p}}\}-1)}] \qquad (2)$$

Fig. 4 *E* shows the catalyzed disulfide reaction of Y401C + W1239C mutant channels. The data are well-described by a nonlinear least-squares best fit curve to Eq. 2, with t_p determined from the time course of solution exchange earlier in the same oocyte. This sort of analysis was undertaken for each of the catalyzed disulfides; Table 1 summarizes the resulting kinetic parameters. The disulfide bond formation rate was fastest for Y401C + G1530C, which we had previously observed to form a high-affinity binding site for Cd^{2+} ions (Bénitah et al., 1996). Although the other rates are slower, all except one (D400C + G1530C) differ by less than an order of magnitude. The concentration of $Cu(phen)_3$ that we used (100 μM) made possible maximum catalysis while avoiding nonspecific effects. Fig. 4 *F* shows the rate of disulfide bond formation (k_{ss}) for Y401C + G1530C mutant channels at various concentrations of $Cu(phen)_3$: k_{ss} increases as the concentration of $Cu(phen)_3$ increases from 10 to 50 μM, but the rate saturates by 100 μM.

If the measured disulfide formation rates indeed reflect thermal protein motions, then k_{ss} should be steeply dependent on temperature. We tested this idea by quantifying the kinetics of inhibition of Y401C + I757C channels by Cu-

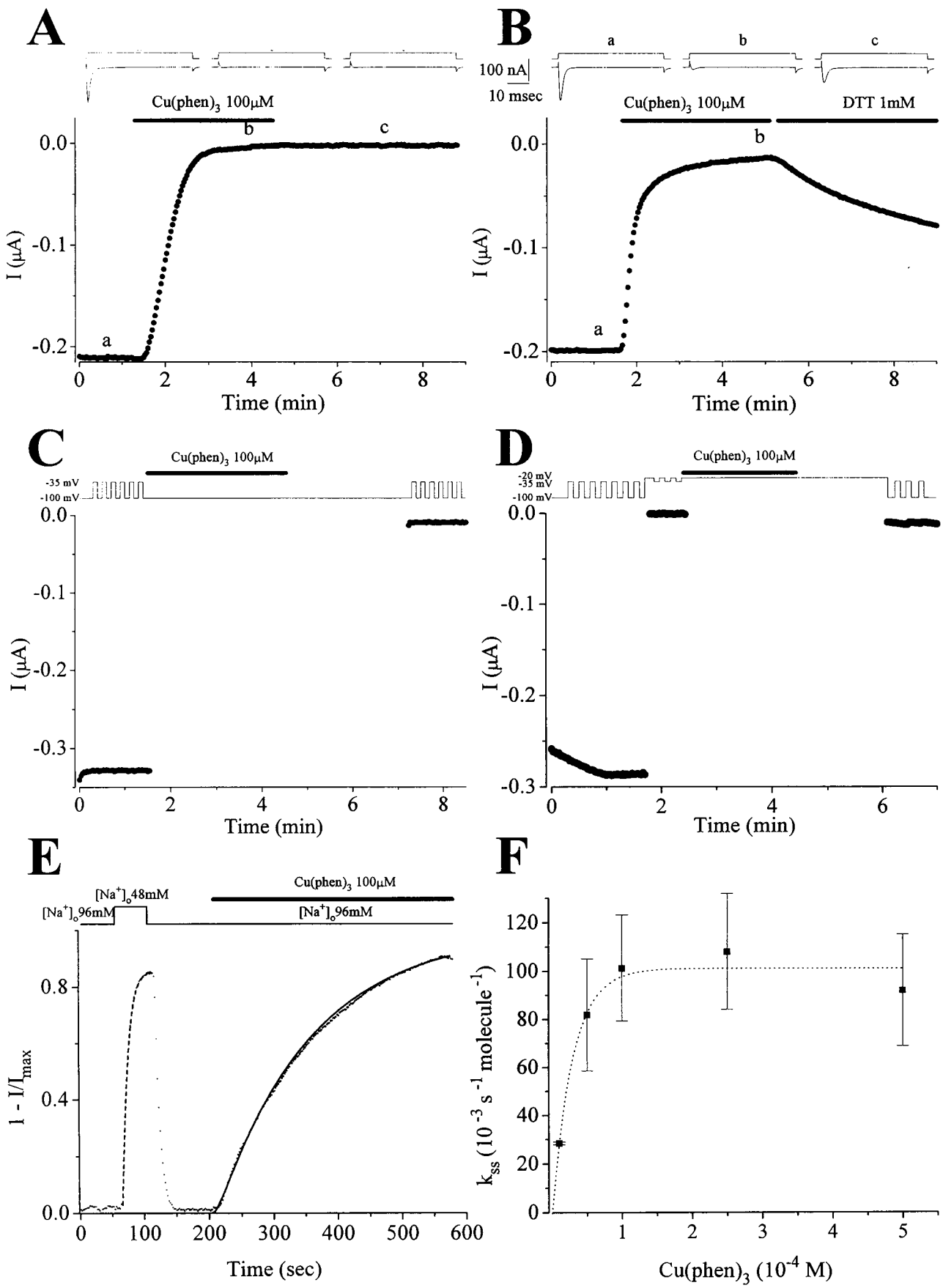
A
Cu(phen)3 100μM
a
b
c
0.0
-0.1
-0.2
I (μA)
0
2
4
6
8
Time (min)
B
a
b
c
100 nA
10 msec
Cu(phen)3 100μM
DTT 1mM
C
Cu(phen)3 100μM
-35 mV
-100 mV
D
-20 mV
-35 mV
-100 mV
E
[Na+]o48mM
[Na+]o96mM
0.8
0.4
1 - I/Imax
0
100
200
300
400
500
600
Time (sec)
F
120
100
80
60
40
20
kss (10-3 s-1 molecule-1)
1
2
3
4
5
Cu(phen)3 (10-4 M)

TABLE 1 Sulfhydryl reactivity and disulfide bond formation rate constants (mean ± SD)

n	k_{SS} ($\times 10^{-3}$ s^{-1} molecule^{-1})	k_2 ($\times 10^{-3}$ s^{-1} molecule^{-1})
Y401C+G1530C n = 13	101.1 ± 46.5	5.3 ± 11.2
D400C+W1531C n = 4	44.9 ± 10.9	10.3 ± 10.6
Y401C+I757C n = 7	36.5 ± 14.5	5.5 ± 6.6
Y401C+W1239C n = 8	23.0 ± 12.0	1.8 ± 2.4
K1237C+G1530C n = 5	9.8 ± 2.3	1.0 ± 0.9
Y401C+D1532C n = 7	8.2 ± 3.5	2.5 ± 6.9
K1237C+W1531C n = 11	7.6 ± 4.1	0.6 ± 0.8
D400C+D1532C n = 8	5.9 ± 1.5	5.3 ± 9.3
D400C+G1530C n = 7	3.5 ± 1.7	3.1 ± 1.9

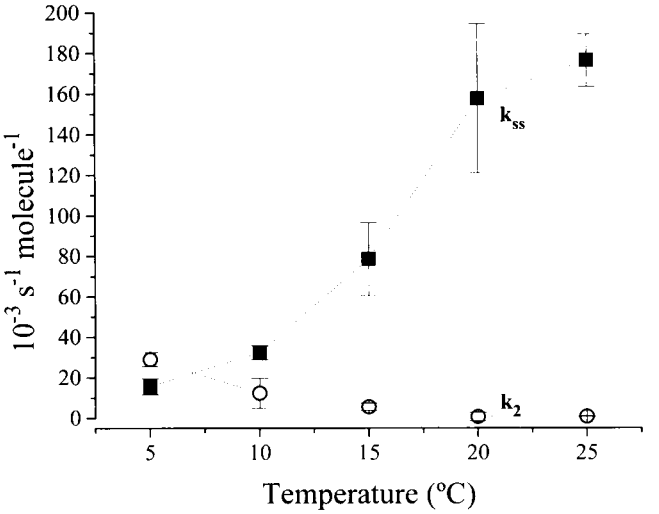

FIGURE 5 Temperature dependence of the disulfide formation rate catalyzed by Cu(II)(1,10-phenanthroline)$_3$. Disulfide formation rate (k_{ss}, ■) and the competing reaction (k_2, ○) of the inhibition of the Y401C + I757C channels by the oxidizing agent are shown as a function of temperature.

(phen)$_3$ at various different temperatures. As illustrated in Fig. 5, the rate of disulfide formation (k_{ss}, *filled squares*) slows markedly with cooling. The Q_{10} of the reaction, calculated between 5° and 25°C, was 5.6. Interestingly, the side reaction with rate k_2 increases with cooling. This may reflect less competition from the disulfide-forming reaction at cooler temperatures, which would increase the availability of free cysteines for the side reaction. Alternatively, the reaction complex may become more stable as diffusion is slowed.

Differences in disulfide formation rates could be explained if the different cysteine pairs are separated by varying distances. Careaga and Falke (1992) used the resolved crystal structure of the D-galactose receptor to calibrate the observed disulfide formation rates as a function of the movement required to bring together the two cysteinyl β carbons. This motion was calculated as the difference between the two cysteine β carbons in the crystal structure and the maximum C^{β}-C^{β} distance (4.6 Å) observed in protein disulfide bonds. Our own values for k_{ss} fall within the mid to upper range of the values observed by Careaga and Falke (1992); taken at face value, these disulfide formation rates would predict motional amplitudes of 5.5–11 Å. Nevertheless, cysteine residues separated by a given equilibrium distance will not necessarily exhibit the same collision frequency at different locations in the same protein, or in different proteins. In fact, disulfide formation rates can change depending on the ligand occupancy of the galactose receptor, even though the equilibrium intercysteine distances do not change significantly (Careaga et al., 1995). Nevertheless, our data provide strong support for the idea that the P segments undergo large internal motions. If the backbones were rigidly constrained, it would be impossible to explain the observation that catalyzed disulfides can form throughout the P segments.

The observed disulfide formation rates also show reassuring internal consistency with the measured Cd^{2+} binding

FIGURE 4 Blockade of double-mutant channels catalyzed by external Cu(II) (1,10-phenanthroline)$_3$. (*A*) An oocyte expressing the double mutant Y401C + G1530C was superfused with ND-96. (*a*) After several pulses, 100 μM Cu(II)(1,10-phenanthroline)$_3$ in ND-96 was applied. The current amplitude is reduced within seconds (*b*) and remains small after washout of the Cu(phen)$_3$ (*c*). (*B*) Disulfide formation was only reversed with 1 mM DTT. Selected current traces recorded at the times indicated by letters *a–c* are shown at the top of *A* and *B*. (*C*) Inhibition of Y401C + G1530C channels by the oxidizing agent in the resting state. The oocyte was held at −100 mV without repetitive stimulation for 3 min during the application of 100 μM Cu(II)(1,10-phenanthroline)$_3$ and for 3 min after washout with ND-96. The current was nearly completely eliminated. (*D*) Cu(II)(1,10-phenanthroline)$_3$ effect on inactivated Y401C + G1530C channels. Pulses from −35 mV to −20 mV before application of Cu(phen)$_3$ demonstrated inactivation of the current. The oxidizing reagent was applied for 2 min and washed out for 2 min while the oocyte was held at −20 mV. Cu(phen)$_3$ at 100 μM irreversibly inhibited the inactivated Na^+ channel. (*E*) Plot of the current through Y401C + W1239C double-mutant channels elicited by depolarizing steps to −20 mV from a holding potential of −100 mV, at a frequency of 0.5 Hz. Currents were recorded in 96 mM extracellular Na^+ (ND-96) for 1 min, then the extracellular Na^+ was decreased to 48 mM. The current was restored by perfusion with ND-96, then 100 μM Cu(II)(1,10-phenanthroline)$_3$ was added to catalyze disulfide bond formation. All current amplitudes are normalized to the initial steady-state current values measured 1 min before the substitution of Na^+. The dashed line is the best-fit single exponential of the solution exchange time course after Na^+ concentration substitution. The solid line is the best fit of Eq. 2 to the data; the rate constants k_{ss} and k_2 for each of the double mutants are given in Table 1. (*F*) Saturation of the catalytic effect of Cu(II)(1,10-phenanthroline)$_3$ on the rate of disulfide bond formation. The rate of disulfide bond formation increases as the concentration of Cu(phen)$_3$ increases, until a maximum value is reached at 100 μM. At higher concentrations no significant change in k_{ss} was observed. The rate constants k_{ss} are determined as in *A*. The dashed line is a monoexponential fit to the data, emphasizing the saturation of the catalytic effect of Cu(phen)$_3$.

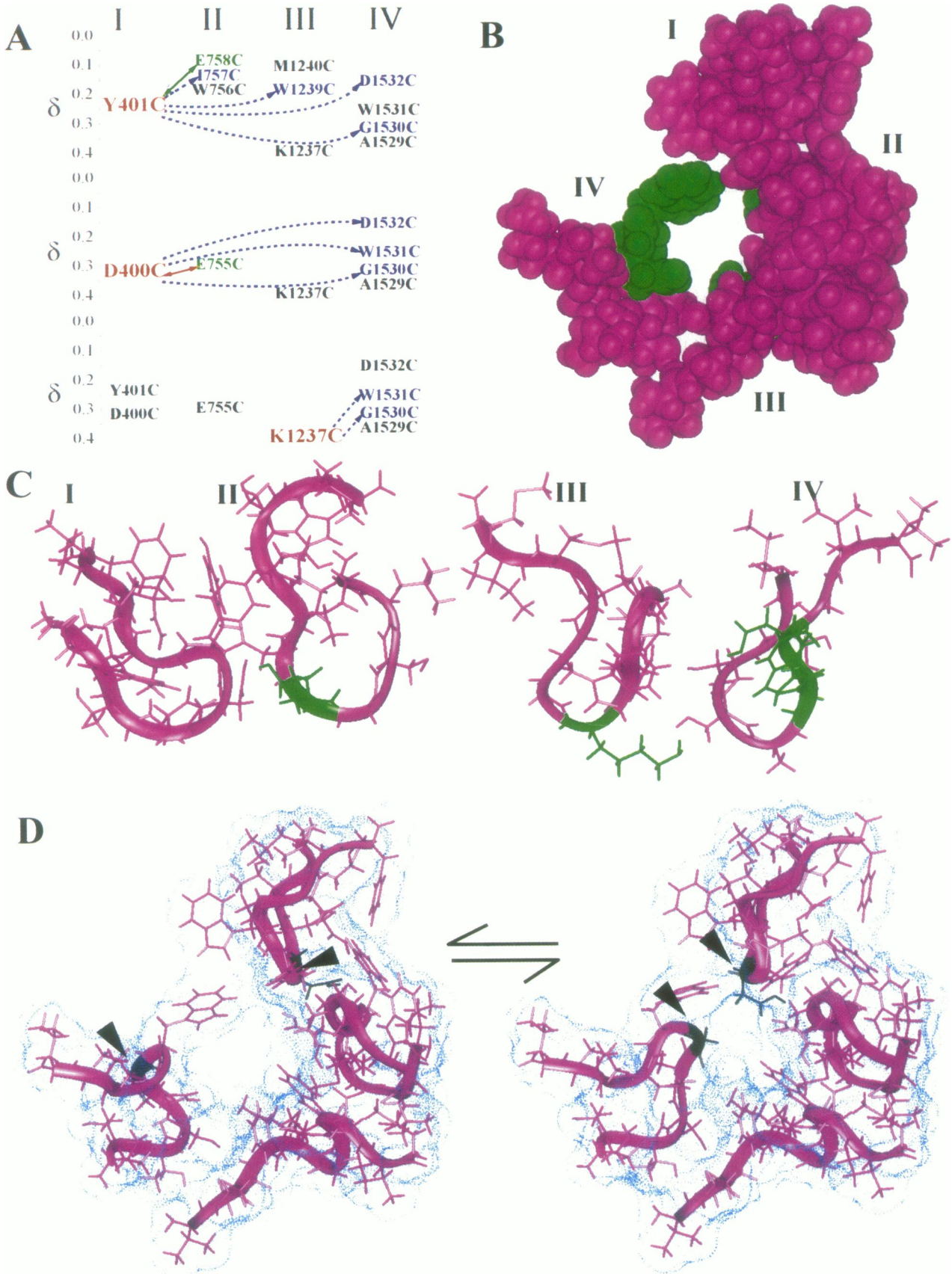
A
I
II
III
IV
δ
Y401C
E758C
I757C
W756C
M1240C
W1239C
D1532C
W1531C
G1530C
A1529C
K1237C
D400C
E755C
Y401C
D400C
E755C
K1237C
B
I
II
III
IV
C
I
II
III
IV
D

affinities. Although the precise values cannot be extrapolated from the galactose receptor (Careaga and Falke, 1992; Careaga et al., 1995), the rank order of proximity of various pairs can be independently deduced to be as follows: 400 + 755 are closest to each other in the structure, 401 + 758 are second, and 401 + 1530 are third. These conclusions are based on the following lines of reasoning. The 400 + 755 and 401 + 758 pairs are both intimately apposed, as they spontaneously form disulfide bonds within the folded protein. When such bonds are broken by exposure to reducing agents, residues 400 and 755 still remain very close to each other, as they bind Cd^{2+} with exceptionally high cooperativity; the Cd^{2+} binding cooperativity is less intense for 401 + 758 channels, so that these two residues are less optimally aligned. The 401 + 1530 pair binds Cd^{2+} cooperatively, but does not form a disulfide spontaneously. The disulfide formation rates (k_{ss}) for the other double mutants, which did not exhibit Cd^{2+} binding cooperativity, were significantly lower.

The results cannot be reconciled with any fixed backbone structure, even allowing for full rotational freedom of the side chains. The patterns of disulfide bonding evident in Fig. 6 *A* show no hint of periodicity of the sort that might be introduced, for example, by sliding movements of α-helices or β-strands. Also notable is the marked asymmetry of the observed reactions. Domains I and II are unique in their ability to form spontaneous disulfides, implying a high collisional frequency between residues in these domains, as expected if the two domains are in fairly constant proximity. In contrast, the domain IV P segment appears to be extraordinarily flexible, forming at least two catalyzed pairs with each of the fulcrum residues.

The results will be easier to reconcile with motions within a pore lined by asymmetrical extended loops, as in the model shown in Fig. 6, *B–D*. This de novo structural model, restricted to the amino acid residues in the P segments (Terlau et al., 1991; Heinemann et al., 1992; Chiamvimonvat et al., 1996a,b; Favre et al., 1996), was developed with the simple linear sequence as the point of departure. First, taking into account the pattern of side-chain accessibility (Pérez-García et al., 1996) and the electrical distances within the transmembrane field of the same residues (Chiamvimonvat et al., 1996a) determined by single-cysteine mutagenesis, a new structural model of the individual P segments of the μ1 Na^+ channel was developed. The specific constraints for intramolecular dimensions related to the spontaneous formation of disulfide bonds spanning domains I and II (Y401C + E758C and D400C + E755C) were then introduced, and the rank order of proximities extrapolated above was obeyed. After each step, the structure was optimized by energy minimization. To generate Fig. 6 *D*, the P segments of domains I and IV were moved so that the β carbons of G1530 and D400 were 4.5 Å apart (sufficiently close for disulfide bond formation in the corresponding double-cysteine mutant), and the model was reminimized. Fig. 6 *B* shows a CPK rendition of the pore viewed from the extracellular surface.

Several notable features emerge. First, as we have argued previously (Chiamvimonvat et al., 1996a), there is marked asymmetry of the P segments and of the pore itself. This asymmetry is consistent with the deduced shape of the pore from organic cation exclusion experiments (Hille, 1971). Second, domains I and II are closely apposed, consistent with the unique ability of pairs involving these two domains to form disulfides spontaneously. In contrast, domains I and IV are relatively distant from each other. In this structure the residues in domain IV that influence selectivity (Chiamvimonvat et al., 1996b) now make up the lining of the narrowest constriction of the pore. The model predicts a narrow passage formed by residues E755, K1237, G1530, W1531, and D1532 (*shown in green*). This region in our model has dimensions of ~4 × 6 Å, comparable to those predicted (Hille, 1971). Fig. 6 *C* shows side views of the resulting structure, with the individual P segments of each domain viewed from the pore lumen.

This structural model emphasizes that the P segments form long, asymmetrical loops, instead of organized β-barrel motifs or α-hairpins, as in previously postulated models (Lipkind and Fozzard, 1994; Guy and Durell, 1995). Such models would be inconsistent with our experimental findings, not only because there is no hint of periodicity in the pattern of single-cysteine accessibility (Perez-Garcia et al., 1996; Chiamvimonvat et al., 1996a), but also because of the marked asymmetries we observe in the thermal backbone motions deduced from disulfide trapping. Furthermore, the extensive motion predicted by our experiments would re-

FIGURE 6 Multiple bonding ability rationalized by a new model of the Na^+ channel pore. (*A*) Spontaneous and catalyzed disulfide bonds of double cysteine mutants in the P segments of the μ1 Na^+ channel. The individual cysteine substitutions that are part of the double mutants in all four P segments (*from left to right*) are plotted as a function of the fractional electrical distances for Cd^{2+} block according to the method of Chiamvimonvat et al. (1996a). The cysteine substitutions Y401C (*top*), D400C (*middle*), and K1237C (*bottom*) were paired with cysteine substitution mutants in the other P segments as shown in each panel. The solid double arrows identify double mutants that spontaneously formed a disulfide bond, and the dashed lines show cysteine pairs that formed disulfide bonds only in the presence of 100 μM Cu(II)(1,10-phenanthroline)$_3$. The unconnected positions showed no redox sensitivity when paired with the indicated fulcrum residue (*boxed*). (*B*) Spatial model of the pore of the μ1 Na^+ channel—a view of the mouth of the channel from the extracellular surface. The structure is shown in a CPK format; the residues in green (E755, K1237, G1530, W1531, and D1532) influence ion selectivity. (*C*) The P sequences of the four domains. The backbone of the P segments is shown in a ribbon configuration, and the amino acid side chains of the critical residues for the selectivity are highlighted in green. The individual P segments are aligned only with respect to their relative depths. An obvious asymmetry of the backbone structure is observed. (*D*) Illustration of motions within the pore of the Na^+ channel. A snapshot of the equilibrium pore structure (*left*) and the minimal translations required to bring the β carbons of the pair of residues G1530 + D400 (*highlighted by arrowheads*) to within 4.5 Å of each other (*right*), permitting disulfide bond formation. The dots represent the solvent-accessible surface of the channel model. The pore is severely constricted when a disulfide bond is formed.

quire significant perturbations of thermodynamically stable structures such as α-helices or β-strands.

Finally, Fig. 6 *D* illustrates an example of the likely movements of the P segments. The left-hand side of the figure shows the time-averaged surface projection of the pore, with the backbone residues rendered as ribbons and the side chains as sticks. In this conformation the β carbons of one pair of residues that can be induced to form a disulfide, G1530 + D400 (*denoted by arrowheads*), are separated by 15.1 Å. In the presence of $Cu(phen)_3$, a disulfide bond forms, trapping the structure in a conformation in which the respective β carbons are separated by less than 4.6 Å and the pore is occluded. Although the distances between residues in the sodium channel equilibrium structure cannot be explicitly constrained by the data from the galactose receptor, the distances in the model are at least compatible with the observed disulfide formation rates, because similar rate/distance ratios have been observed in this protein of known structure (Careaga and Falke, 1992). In addition, the model is consistent with all of the published accessibility data for single-cysteine mutants, as well as with the fractional electrical distances measured from single-channel recordings of Cd^{2+} block (Chiamvimonvat et al., 1996a).

Flexible loops are a recurrent structural theme in enzyme active sites and impart the advantages of optimal arrangement of residues involved in catalysis. The Na^+ channel pore catalyzes the selective, yet highly efficient transport of Na^+ across the cell membrane. Our data provide additional support for the hypothesis that flexible loops form the structural basis of the permeation pathway in the voltage-dependent Na^+ channel. The idea that small internal motions may be required for ion selectivity is not new; indeed, it is implicit in the close-fit hypothesis of Mullins (1959). Side-chain flexibility and ligand competition figure prominently in current concepts of calcium channel permeation (Kuo and Hess, 1993; Chen et al., 1996). The motions that we have inferred are larger and more extreme: they are predicted to involve backbone distortions of several angstroms. The present findings necessitate that flexibility be considered as a potential determinant of selective ion flux.

We thank D. Romashko for advice regarding data analysis and A. Mendez-Fitzwilliam for technical assistance with mutagenesis.

Supported by the National Institutes of Health and by the American Heart Association (Maryland Affiliate).

REFERENCES

Armstrong, C. M. 1989. Reflections on selectivity. *In* Membrane Transport: People and Ideas. D. C. Tosteson, editor. Waverly Press, Baltimore, MD. 261–274.

Bénitah, J.- P., G. F. Tomaselli, and E. Marban. 1996. Adjacent pore-lining residues within sodium channels identified by paired cysteine mutagenesis. *Proc. Natl. Acad. Sci. USA.* 93:7392–7396.

Brooks, C. L., M. Karplus, and B. M. Pettitt. 1988. Proteins: a theoretical perspective of dynamics, structure, and thermodynamics. *In* Advances in Chemical Physics, Vol. 71. I. Prigogine and S. A. Rice, editors. Interscience Publication.

Careaga, C. L., and J. J. Falke. 1992. Thermal motions of surface α-helix in D-galactose chemosensory receptor: detection by disulfide trapping. *J. Mol. Biol.* 226:1219–1235.

Careaga, C. L., J. Sutherland, J. Sabeti, and J. J. Falke. 1995. Large amplitude twisting of an interdomain hinge: a disulfide trapping study of the galactose-glucose binding protein. *Biochemistry.* 34:3048–3055.

Chen, X.-H., I. Bezprozvanny, and R. W. Tsien. 1996. Molecular basis of proton block of the L-type Ca^{2+} channels. *J. Gen. Physiol.* 108:363–374.

Chervitz, S. A., C. M. Lin, and J. J. Falke. 1995. Transmembrane signaling by the aspartate receptor: engineered disulfides reveal static regions of the subunit interface. *Biochemistry.* 34:9722–9733.

Chiamvimonvat, N., M. T. Pérez-García, R. Ranjan, E. Marban, and G. F. Tomaselli. 1996a. Depth asymmetries of the pore-lining segments of the Na^+ channel revealed by cysteine mutagenesis. *Neuron.* 16:1037–1047.

Chiamvimonvat, N., M. T. Pérez-García, G. F. Tomaselli, and E. Marban. 1996b. Control of ion flux and selectivity by negatively charged residues in the outer mouth of rat sodium channels. *J. Physiol. (Lond.).* 491: 51–59.

Eisenman, G., and S. Krasne. 1975. The ion selectivity of carrier molecules, membranes and enzymes. *In* MTP International Review of Science, Biochemistry Series, Vol. 2. C. F. Fox, editor. Butterworths, London. 27–59.

Falke, J. J., and D. E. Koshland. 1987. Global flexibility in a sensory receptor: a site directed disulfide approach. *Science.* 237:1596–1600.

Favré, I., E. Moczydlowski, and L. Schild. 1996. On the structural basis for ionic selectivity among Na^+, K^+ and Ca^{2+} in the voltage-gated sodium channel. *Biophys. J.* 71(6):3110–3125.

French, R. J., E. Prusak-Sochaczewski, G. W. Zamponi, S. Becker, A. Shavantha Kularatna, and R. Horn. 1996. Interactions between a pore-blocking peptide and the voltage sensor of the sodium channel: an electrostatic approach to channel geometry. *Neuron.* 16:407–413.

Guy, H. R., and S. R. Durell. 1995. Structural model of Na^+, Ca^{2+}, and K^+ channel. *In* Ionic Channels and Genetic Diseases, Vol. 50, Society of General Physiologists Series. D. C. Dawson and R. A. Frizzell, editors. Rockefeller University Press, New York. 1–16.

Heinemann, S. H., H. Terlau, W. Stühmer, K. Imoto, and S. Numa. 1992. Calcium channel characteristics conferred on the sodium channel by single mutations. *Nature.* 356:441–443.

Hille, B. 1971. The permeability of the sodium channel to organic cations in myelinated nerve. *J. Gen. Physiol.* 58:599–619.

Hille, B. 1992. Ionic Channels of Excitable Membranes, 2nd Ed. Sinauer Associates, Sunderland, MA. 337–389.

Isom, L. L., K. S. De Jongh, D. E. Patton, B. F. X. Reber, J. Offord, H. Charbonneau, K. Walsh, A. L. Goldin, and W. A. Catteral. 1992. Primary structure and functional expression of the β1 subunit of the rat sodium channel. *Science.* 256:839–842.

Kamp, T. J., M. T. Pérez-García, and E. Marban. 1996. Enhancement of ionic current and charge movement by coespression of calcium channel β1a subunit with α1c subunit in a human embryonic kidney cell line. *J. Physiol. (Lond.).* 492:88–96.

Krovetz, H. S., H. M. A. VanDongen, and A. M. J. VanDongen. 1997. Atomic distance estimates from disulfides and high-affinity metal-binding sites in K^+ channel pore. *Biophys. J.* 72:117–126.

Kuo, C. C., and P. Hess. 1993. Characterization of the high-affinity Ca^{2+} binding sites in the L-type Ca^{2+} channel pore in rat phaeochromocytoma cells. *J. Physiol. (Lond.).* 466:657–682.

Levitt, M. 1989. Molecular dynamics of macromolecules in water. *Chim. Scripta.* 29A:197–203.

Lipkind, G. M., and H. A. Fozzard. 1994. A structural model of tetrodotoxin and saxitoxin binding site of the Na^+ channel. *Biophys. J.* 66:1–13.

Liu, Y., M. E. Jurman, and G. Yellen. 1996. Dynamic rearrangement of the outer mouth of a K^+ channel during gating. *Neuron.* 16:859–867.

Mullins, L. J. 1959. An analysis of conductance changes in squid axon. *J. Gen. Physiol.* 42:817–829.

Oae, S. 1991. Organic Sulfur Chemistry: Structure and Mechanism. J. T. Doi, editor. CRC Press, Boca Raton, FL. 203–281.

Pérez-García, M. T., N. Chiamvimonvat, E. Marban, and G. F. Tomaselli. 1996. Structure of the sodium channel pore revealed by serial cysteine mutagenesis. *Proc. Natl. Acad. Sci. USA.* 93:300–304.

Pérez-García, M. T., N. Chiamvimonvat, R. Ranjan, J. R. Balser, E. Marban, and G. F. Tomaselli. 1997. Mechanisms of sodium/calcium selectivity in sodium channels probed by cysteine mutagenesis and sulfhydryl modification. *Biophys. J.* 72:989–996.

Srinivasan, N., R. Sowdhamini, C. Ramakrishnan, and P. Balaram. 1990. Conformations of disulfide bridges in protein. *Int. J. Pept. Protein Res.* 36:147–155.

Terlau, H., S. H. Heinemann, W. Stühmer, M. Pusch, F. Conti, K. Imoto, and S. Numa. 1991. Mapping the site of block by tetrodotoxin and saxitoxin of sodium channel II. *FEBS Lett.* 293:93–96.

Tomaselli, G. F., N. Chiamvimonvat, H. B. Nuss, J. R. Balser, M. T. Pérez-García, R. H. Xu, D. W. Orias, P. H. Backx, and E. Marban. 1995. A mutation in the pore of the sodium channel alters gating. *Biophys. J.* 68:1814–1827.

Trimmer, J. S., S. S. Copperman, S. A. Tomiko, J. Zhou, S. M. Crean, M. B. Boyle, R. G. Kallen, Z. Sheng, R. L. Barchi, F. J. Sigworth, R. H. Goodman, W. S. Agnew, and G. Mandel. 1989. Primary structure and functional expression of α mammalian skeletal muscle sodium channel. *Neuron.* 3:33–49.

Tsushima, R. G., R. A. Li, and P. H. Backx. 1997. Altered ionic selectivity of the sodium channel revealed by cysteine mutations within the pore. *J. Gen. Physiol.* 109:463–475.

Weiner, M. P., K. A. Felts, T. G. Simcox, and J. C. Brama. 1993. A method for the site-directed mono- and multi-mutagenesis of double stranded DNA. *Gene.* 126:35–41.

Wells, J. A. 1990. Additivity of mutational effects in proteins. *Biochemistry.* 29:8509–8512.

Yamagishi, T., M. Janecki, E. Marban, and G. F. Tomaselli. 1997. Topology of the P segments in the sodium channel pore revealed by cysteine mutagenesis. *Biophys. J.* 73:195–204.

Yang, N., A. L. George, and R. Horn. 1996. Molecular basis of charge movement in voltage-gated sodium channels. *Neuron.* 16:113–122.

Zhang, H.-J., Y. Liu, R. D. Zühlke, and R. H. Joho. 1996. Oxidation of an engineered pore cysteine locks a voltage-gated K^+ channel in a nonconducting state. *Biophys. J.* 71:3083–3090.